Increase the rigidity and hydrophobicity of perovskite by a molecular design

Increase the rigidity and hydrophobicity of perovskite by a molecular design

Yabing Qi*
Energy Materials and Surface Sciences Unit (EMSSU)
Okinawa Institute of Science and Technology Graduate University (OIST)
1919-1 Tancha, Onna-son, Kunigami-gun
Okinawa, Japan 904-0495
*E-mail: Yabing.Qi@OIST.jp

Organic-inorganic hybrid perovskite solar cells are rising as the most promising next generation solar cells due to their excellent efficiency and low-cost fabrication. Organic components in A-site (ABX_3) play an important role in the structure of perovskite materials. For example, it has been reported that the introduction of dimethylamine (DMA) or formamidine (FA) into perovskite structure results in the phase change from tetragonal to cubic[1-3]. However, up to now, the relation between the introduced molecules and performance of perovskite solar cells is unclear.

Recently, Chen et al. investigated the modification of perovskite properties by incorporating secondary amine into the $MAPbI_3$ structure, i.e., dimethylamine (DMA)[4]. Theoretical simulation was conducted to investigate the impact of the introduction of DMA to the structural property of the perovskite. The small change of the average Pb-I bond length under 0 K and 300 K suggests that the introduction of DMA can increase the rigidity of the perovskite structure (Figure1(a-b)). Furthermore, electrochemical strain microscopy (ESM) was used to map the structural stability of films by comparing the transient response which can be an estimation of ion diffusion rate between **DMA0.11**($MA_{0.89}DMA_{0.11}PbI_3$) and **MA1**($MAPbI_3$). The relaxation time for **DMA0.11** was 50% larger than that of **MA1**, suggesting inhibited ion diffusion in **DMA0.11**. This finding confirms that the inclusion of DMA leads to increase of the structural rigidity (Figure2(a-b)).

The authors then investigated the influence of structural stiffness on the formation of defects, e.g., they calculated the defect formation energy of the structure with and without DMA. Schottky defect MAI vacancy, PbI_2 vacancy, and antisite Pb_I defects were studied and it is find that the defect formation energy are all improved after the incorporation of DMA(Figure1(c-d)). Besides, the interface of the device is important due to serious carrier recombination. As shown in Figure1(f-g), Ab initio molecular dynamics (AIMD) was conducted to compare the interface of NiO/**MA1** and NiO/**DMA0.125**($MA_{0.875}DMA_{0.125}PbI_3$). Due to the better lattice match at the NiO/**DMA0.125** interface, the radial distribution functions for both the Pb-I bond and Ni-O bond show a higher and narrower peak, indicating the higher quality of the NiO/**DMA0.125** interface. Then the photoluminescence (PL) spectra were measured for **DMA0.11** and **MA1**. The PL intensity of **DMA0.11** is almost 2 times higher than **MA1**, and the PL decay lifetime of the **DMA0.11** is also much longer than that of **MA1**, confirming reduced trap states after the incorporation of DMA.

Apart from the reduction of defects, compared with the primary amine MA, the secondary amine DMA can increase the steric hindrance (Figure2(d)) for water adsorption, as evidenced by DFT simulation (Firure1(e)), and water contact angle measurement. As a result, the **DMA0.11** film shows no obvious decrease in the optical density at 750 nm under a relative humidity (RH) of 80 ± 5% after tracking the evolution of the absorption spectra for over 10 days, while **MA1**'s optical density decreased to 80% of its original value (Figure2(c)).

By introducing the secondary amine molecule DMA, the PSCs achieved a power conversion efficiency of 21.6%. The certified efficiency is 20.8%, which is the highest among inverted PSCs based on NiO substrates. Furthermore, the encapsulated devices maintain over 80% of their original efficiency following 800 h of operation at the maximum power point.

This work clarifies the relationship between the molecular structure and optoelectronic properties of perovskite, and sheds some light on the strategy to obtain both high efficiency and stability of PSCs.

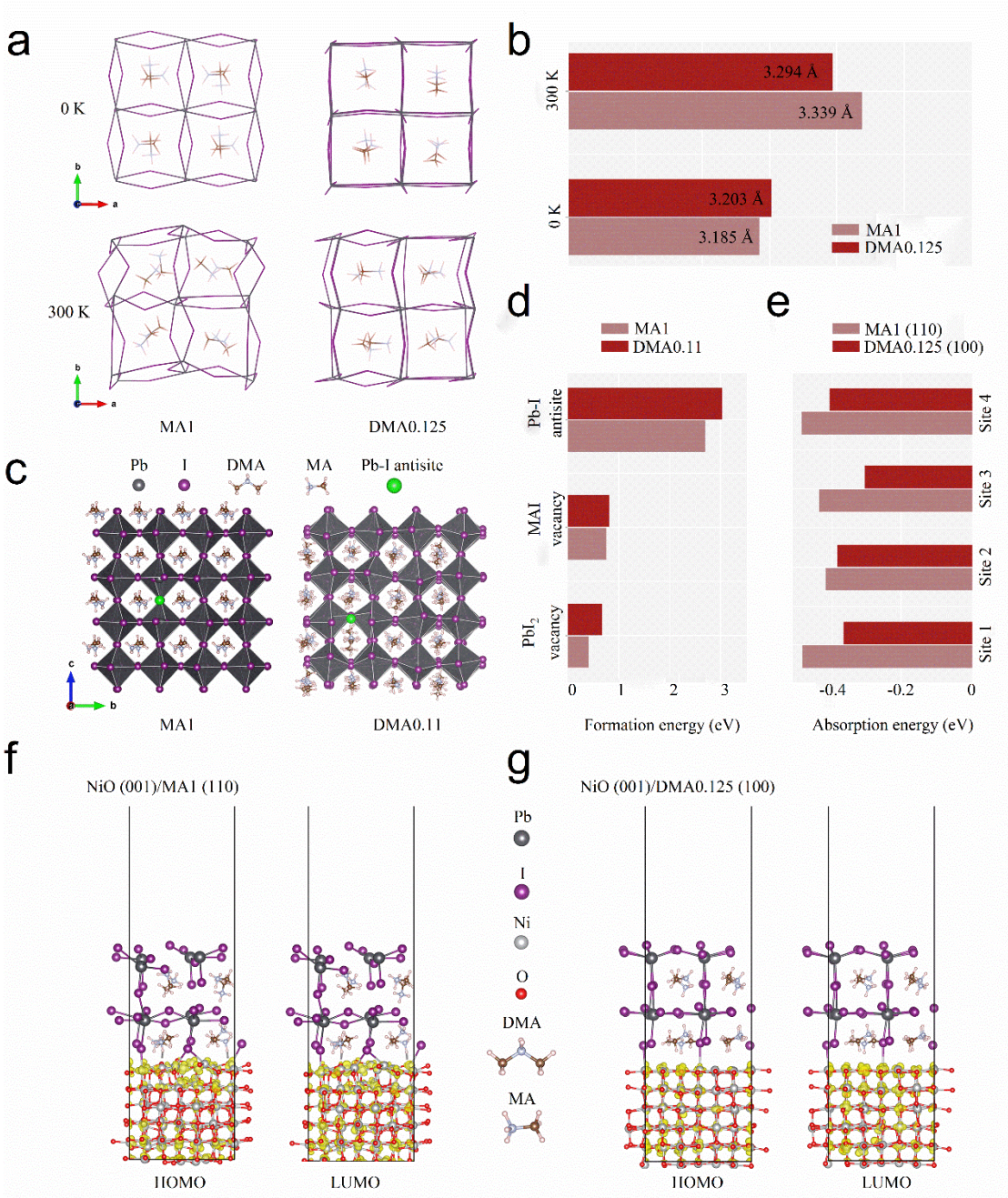

Figure 1. (a-b) The comparison of the structure change under 0 K and 300 K for **MA1** and **DMA0.125.** (c-d) defect formation energy calculation for **MA1** and **DMA0.11**. (e) water absorption energy calculation for **MA1** and **DMA0.125**. (f-g) interface AIMD calculation for NiO/**MA1** and NiO/**DMA0.125**. Reprinted with permission from Ref. [4], Copyright 2019 Wiley-VCH Verlag GmbH & Co. KGaA, Weinheim.

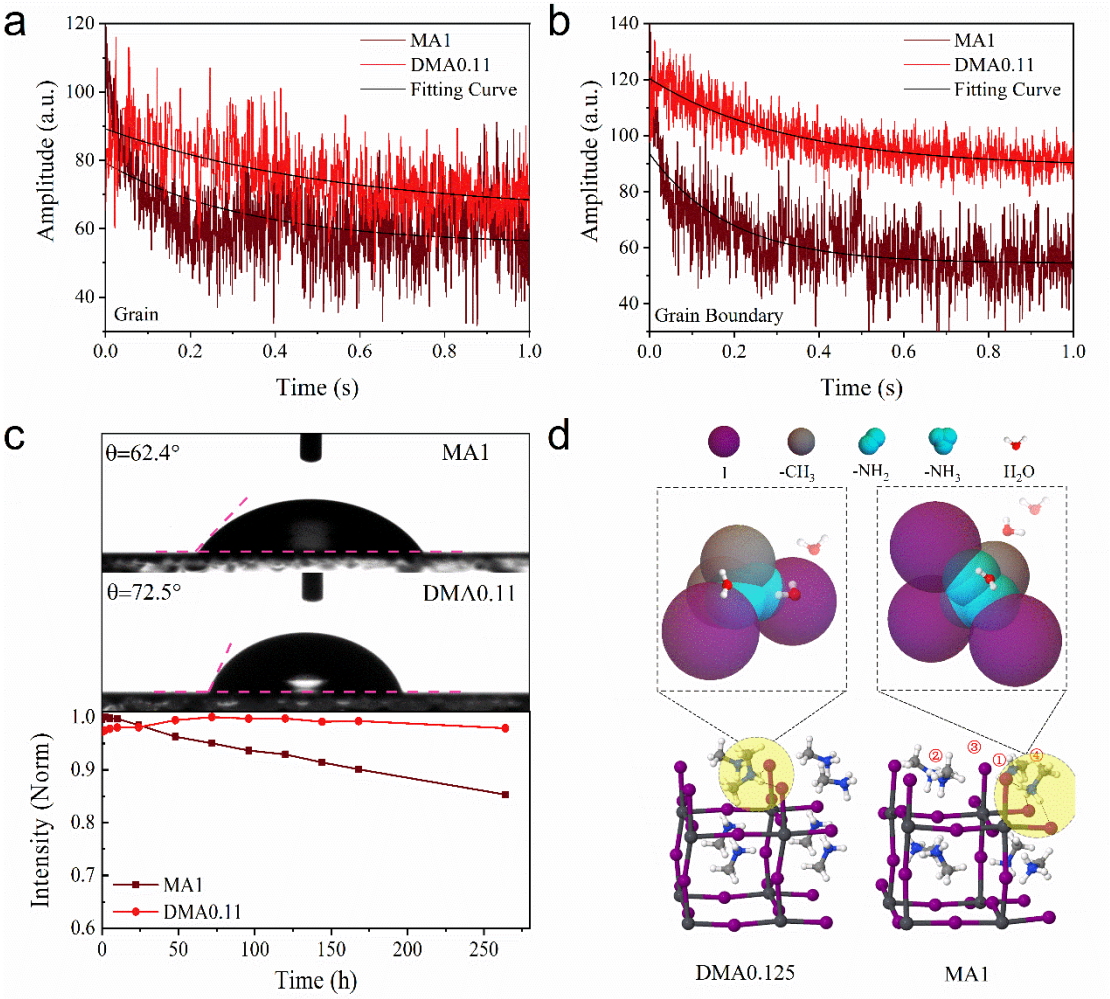

Figure 2. (a-b) The experimental ESM amplitude of grain and grain boundary versus time for **MA1** and **DMA0.11** measured under a bias of -2 V. (c) The static water contact angle measurement of **MA1** and **DMA0.11** perovskite films. (d) calculated water absorption sites and the illustration of the steric hindrance difference between **MA1** and **DMA0.125**. Reprinted with permission from Ref. [4], Copyright 2019 Wiley-VCH Verlag GmbH & Co. KGaA, Weinheim.

Acknowledgments

The author acknowledges the support from the Energy Materials and Surface Sciences Unit of the Okinawa Institute of Science and Technology Graduate University, the OIST R&D Cluster Research Program, the OIST Proof of Concept (POC) Program, and JSPS KAKENHI (JP18K05266).

References:

[1] Lee MV, Raga SR, Kato Y, et al. Transamidation of dimethylformamide during alkylammonium lead triiodide film formation for perovskite solar cells. Journal of Materials Research, 2017, 32: 45-55

[2] Weller MT, Weber OJ, Frost JM, et al. Cubic perovskite structure of black formamidinium lead iodide, α-[HC(CH2)]PbI3, at 298 k. The journal of physical chemistry letters, 2015, 6: 3209-3212

[3] Shi Z, Zhang Y, Cui C, et al. Symmetrization of the crystal lattice of $MAPbI_3$ boosts the performance and stability of metal–perovskite photodiodes. Advanced materials, 2017, 29:

1701656
[4] Chen H, Wei Q, Saidaminov MI, et al. Efficient and stable inverted perovskite solar cells incorporating secondary amines. Advanced materials, 2019, 1903559